Transport properties of an armchair carbon nanotube with a double vacancy under stretching

2008 J. Phys.: Condens. Matter 20 345225

(http://iopscience.iop.org/0953-8984/20/34/345225)

J. Phys.: Condens. Matter **20** (2008) 345225 (6pp) doi:10.1088/0953-8984/20/34/345225

Transport properties of an armchair carbon nanotube with a double vacancy under stretching

Zi Li[1,4], Chong-Yu Wang[1,2], Xu Zhang[1], San-Huang Ke[3] and Weitao Yang[3]

[1] Department of Physics, Tsinghua University, Beijing 100084, People's Republic of China
[2] The International Centre for Materials Physics, Chinese Academy of Sciences, Shenyang 110016, People's Republic of China
[3] Department of Chemistry, Duke University, Durham, NC 27708-0305, USA

E-mail: lizi@mails.tsinghua.edu.cn

Received 27 June 2008, in final form 22 July 2008
Published 6 August 2008
Online at stacks.iop.org/JPhysCM/20/345225

Abstract
Structural properties of metallic single-walled carbon nanotubes with a double vacancy under stretching are studied by using a multiscale hybrid energy density method. Based on the optimized structure, the single-particle Green function method is then used to investigate the transport property. It is found that a reconstruction of the structure occurs with an increase of the imposed axial force, which alters the transmission function around the Fermi energy and will reduce the current. This reconstruction cannot be found by running a molecular dynamics simulation without a quantum description.

1. Introduction

Carbon nanotubes (CNTs) have become very promising one-dimensional materials in nanoscience. The tremendous potential for technological applications has thrust them into one of the hottest areas of research activities [1–3]. Some recent observations of strong coupling between mechanical deformation and electrical behavior [4] show that CNTs have exciting electromechanical properties. Various experimental [5–7] and theoretical [8–12] studies have been attracted to explore the correlation between the mechanical deformation and the change of electric transport in CNTs. Defects can appear at the stage of CNT growth, or later on during device or composite production. Moreover, defects in CNTs can be created deliberately by chemical treatment [13] or by irradiation [14, 15]; controlling their density can be achieved by manipulating the electronic characteristics of the CNTs. Defects (such as topological defects, tube–tube junctions and vacancies) and coherent electric conductance have been studied both experimentally and computationally [8, 9, 16, 17].

The conductance of a one-dimensional conductor is known to have a simple form according to Landauer's formula [18], i.e. the number of conducting channels times the conductance quantum ($G_0 = 2e^2/h$) [19]. An armchair single-walled CNT is a metallic nanowire with two electronic energy bands crossing at the Fermi level and contributing two conductance quanta ($2G_0$) to its conductance [20–22]. This quantized conductance could be changed by local defects.

Double vacancy (produced by removing two neighboring atoms in CNT) is one of the important defects in CNTs. Its effects on electron transport have been studied by different experiments [17, 23, 24] and theoretical simulations [12, 16, 17, 25]. In the experiment of Navarro *et al* [17], it was found that a low density (0.03%) of double vacancy can cause an increase, by three orders of magnitude, in the resistance of a single-walled CNT. Although the effect of double vacancy has been studied extensively, its detailed structure and transport properties under an external stress have not been fully understood.

In this work, we consider an armchair single-walled CNT with a double vacancy and study the variation of its transport property with an increasing imposed axial external force. Our structural model of CNT with a double vacancy consists of thousands of atoms, with external forces imposed at the two ends. A multiscale method combined density functional theory (DFT) and atomistic simulations is applied to optimize the

[4] Author to whom any correspondence should be addressed.

structures. Since the conductance sensitively depends on the local structural defects and the defects are coupled with the long range environment in our systems, the multiscale modeling is appropriate. The rest of our paper is organized as follows. In section 2, the structural models and computational details are described. The results are given and discussed in section 3. Finally we summarize our work in section 4.

2. Models and calculation method

2.1. Multiscale hybrid method

In the hybrid energy density method (EDM) [26, 27], a system is partitioned into three subsystems: a quantum mechanics (QM) region, a classical molecular dynamics (MD) region, where DFT and classical MD simulations are performed, respectively, and a transition (TR) region used to accommodate the coupling of the former two regions. The coupling Hamiltonian of the transition region is constructed by using the structural energy and weight parameters. The force on each atom in the entire system can be obtained in terms of the total energy expression [27]:

$$F_{i\in\mathrm{QM}} = F_i^{\mathrm{DFT}},$$

$$F_{j\in\mathrm{MD}} = F_j^{\mathrm{MD}},$$

$$F_{k\in\mathrm{TR}} = \omega_k^{\mathrm{QM}} F_k^{\mathrm{DFT}} + \omega_k^{\mathrm{MD}} F_k^{\mathrm{MD}}$$

where F_l^{DFT} and F_l^{MD} describe the force acting on the atom, and are calculated from DFT and MD, respectively. ω_l^{QM} and ω_l^{MD} represent the weights of the contributions from the DFT and MD simulations in the transition region, respectively. They are related by $\omega_l^{\mathrm{QM}} + \omega_l^{\mathrm{MD}} = 1$. Here we choose linear-form weight parameters in the transition region which are shown in figure 1. Based on the calculation of the force on each atom, we can perform the structural optimization for the entire system.

For the DFT part of the hybrid simulation, we use the DMol3 program [28]. The electronic wavefunction is expanded in a localized atom-centered basis set. All-electron calculations are performed with a double numerical polarized basis set (the most complete set available in the code) and the gradient-corrected PBE energy functional [29]. For the atomistic simulation, the Tersoff-type many-body potential [30, 31] with the parameters given by Brenner [32] is used for the covalent interactions between carbon atoms. This potential has been widely used to simulate diamond, graphite, CNTs and many hydrocarbon complexes [33–36].

For the structure model, we consider a (5, 5) armchair single-walled CNT with a double vacancy (CNT-DV), which consists of 9988 atoms, as shown in figure 1. To stretch the CNT, we impose an axial external force at each of the two ends. According to the partition in the hybrid method, the CNT-DV system is divided into three regions: the QM, transition and MD regions, with the double vacancy locating at the middle of the QM region, as shown in figure 1. The QM region contains 48 atoms and the two transition regions both contain 70 atoms. The rest of the atoms belong to the MD region. The optimization of the entire structure is performed by minimizing

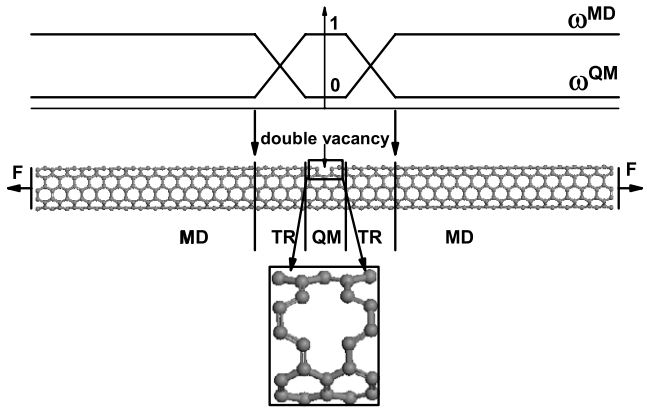

Figure 1. The schematic structure model for the multiscale calculation. The weight function is also shown.

the forces on the atoms to be less than 0.06 eV Å^{-1}. Then we intercept a central section with 228 atoms of the CNT as the conductor of interest, which contains the defect in the middle. The atoms out of the section in an infinite open system are derived from an ideal bonding arrangement. This central part will be used for the further first-principles electronic structure and transport calculations.

2.2. Single-particle Green function method

We adopt the GF method [19, 37] combining a Landauer formula with an *ab initio* DFT electronic structure calculation to investigate the electron transport through the nanotube. In our model for transport calculation, the left and right electrodes both have a unit cell of 40 carbon atoms. The (unbiased) self-consistent Kohn–Sham Hamiltonian of the device region and the self-energies from the two semi-infinite nanotube leads are used to construct a single-particle Green function from which a new density matrix for a finite bias voltage is calculated, which updates the Kohn–Sham Hamiltonian of the device region. The procedure continues on until the nonequilibrium density matrix is converged. Then the transmission coefficient at any energy is calculated in terms of the converged Green function, whose energy integration gives the current for the specific bias voltage. The detailed computational techniques have been described previously [37].

For the DFT electronic structure calculation, we make use of the optimized Troullier–Martins pseudopotentials [38] for the atomic cores. The PBE version of the generalized gradient approximation (GGA) [29] is used for the electron exchange and correlation. The wavefunctions are expanded using a numerical single-zeta (SZ) basis set [39]. We also tested the single-zeta plus polarization (SZP) basis set and the transmission function and the conductance changed little, because the coupling is in the strong coupling limit [40].

3. Results and discussion

3.1. The structure optimization using the EDM method

The multiscale hybrid method is used to relax the structures of the CNT-DV systems under external forces of 0 and

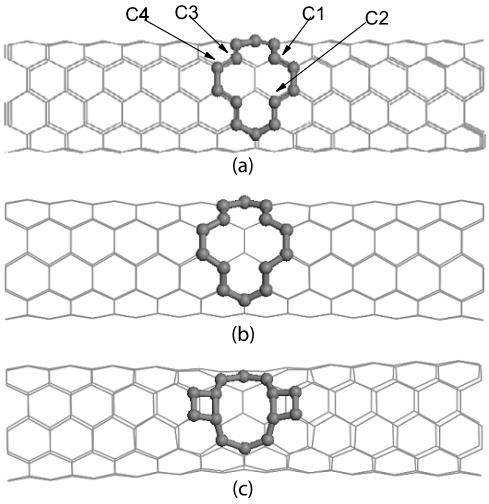

Figure 2. Structures of the CNT-DV systems optimized by the multiscale method under (b) 0 nN and (c) 50 nN. (a) is the unoptimized structure under 0 nN.

50 nN, using the DMol3 program and Tersoff potential. The different external forces lead to very different structures near the vacancy. The structure of the central part (containing 228 atoms) is plotted in figure 2. We can see that for 0 nN the atoms near the double vacancy do not form new bonds and their positions change only little. However, for 50 nN they form new bonds along the circumference of the CNT. For the former system, the distance between C1 and C2 (labeled in figure 2) is 2.93 Å, and that between C1 and C3 is 2.46 Å, both being much longer than the common C–C bond length of 1.42 Å [3]. For the latter system, the distance between C1 and C2 is 1.58 Å, and the one between C1 and C3 is 3.53 Å, indicating that a new chemical bond is formed between C1 and C2.

We then optimize the CNT-DV systems under a series of external forces between 0 and 50 nN and find that the critical force for the transition is between 33 and 34 nN. We also carefully tested our result with different sizes of the transition region. With a larger transition region, say 90 atoms, the critical force does not change, while with a smaller transition region, 30 atoms, the critical force changes to 34–35 nN. We also calculated the CNT-DV systems only using the molecular dynamics with a Tersoff potential and found no reconstruction for a wide range of external forces, from 0 to 80 nN. These indicate that the use of the hybrid method in this work is essentially important and our choice for the size of the transition region is reasonable and necessary.

3.2. Electronic structure calculation for the central part

After the optimization, we use the first-principles DMol3 program to study in more detail the electronic structure of the central part of the CNT-DV systems under 0 and 50 nN external forces. The calculated charge density difference of the two systems are plotted in figure 3. The bonding properties can be seen clearly: the 0 nN system forms no new bonds near the vacancy while the 50 nN system forms new bonds along the circumference of the tube.

The Mayer bond orders [41] are also calculated. For the 0 nN system, the bond order of C1 and C2 is 0.02, meaning no bonding interaction between them, while the one of C1 and C3 is 0.69, being half of the value of the common C–C bond in CNTs. This means that there is a small trend to form a new bond between C1 and C3, but it is too small to be seen in the charge density difference. For the 50 nN system, the bond order of C1 and C2 is 1.02, while the value of C1 and C3 is 0.01, indicating that a common C–C bond is formed between C1 and C2.

In figure 4 we show the P_z component (the z axis is vertical to these atoms) of the local DOS (LDOS) of the atoms around the vacancy. We can see that the C4 atom in the 50 nN system has a local state near the Fermi energy, while in the 0 nN system the LDOS of C4 is similar to that of the atoms far away. In contrast to C4, the LDOS of C1 atoms for both of the 0 and 50 nN systems have local states and are very different from that of the atoms far away. These imply a larger break of the conjugated π bonds and a stronger scattering in electron transport in the 50 nN system.

The highest occupied molecular orbital (HOMO) of the 0 and 50 nN systems is also shown in figure 4. We can see that, for the 50 nN system, the HOMO is mainly localized around the double vacancy due to the large structural deformation. In contrast, the HOMO of the 0 nN system is much more extended. These results are consistent with the LDOS analysis above.

From the LDOS we also calculate the structural energy of the atoms in the central part. The structural energy is defined as follows:

$$E_s(i) = \int_{-\infty}^{E_F} E \cdot \mathrm{LDOS}(i, E)\,\mathrm{d}E$$

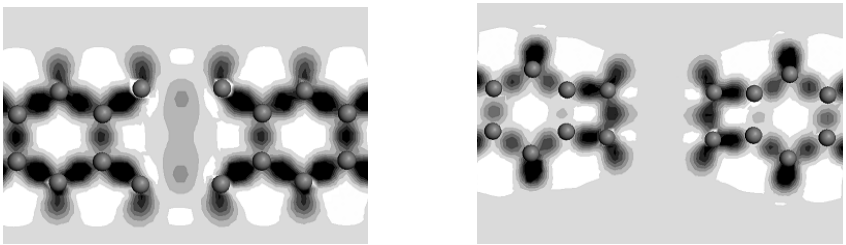

Figure 3. Charge density difference of the CNT-DV systems under (a) 0 nN and (b) 50 nN. The darker spot represent the larger charge density than that of the free atom, which means a stronger bonding.

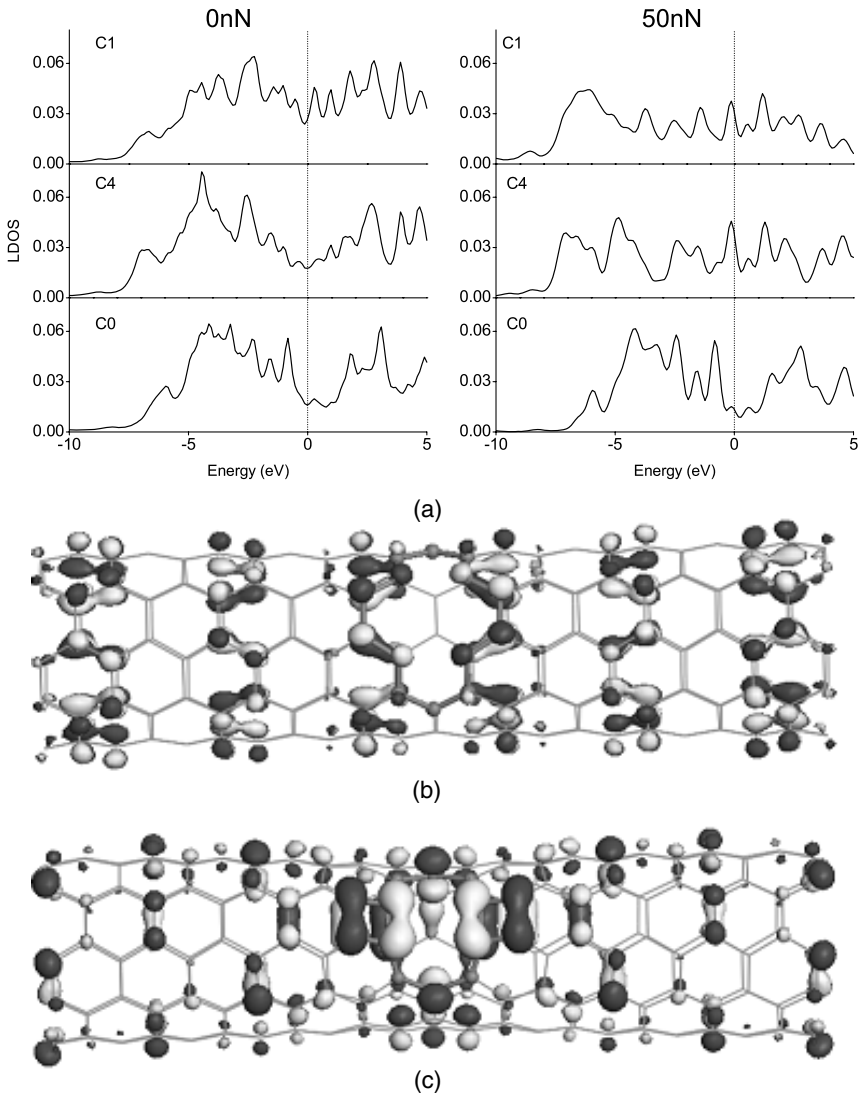

Figure 4. (a) shows the P_z component of LDOS of the atoms near the vacancy. The atoms C1 and C4 are denoted in figure 2(a). C0 is an atom far away from the defect. The Fermi energy is set to be zero. (b) and (c) are the HOMO orbitals of the CNT-DV systems under 0 and 50 nN, respectively. The white and black colors are used to denote the positive and negative lobes of the orbitals.

where i denotes the atom index and E_F is the Fermi energy. The structural energy contains the information from electrons of a specific atom, and the atoms may have different values of structural energy in different environments. In figure 5, we give the average value of the structural energy for each layer of the CNT. We can see that for both 0 and 50 nN systems the average structural energy tends to be a constant three layers away from the vacancy. This indicates that the effect of the defect we considered here is very localized. Note that the value in the edges changes a lot, due to the dangling bonds.

3.3. Transport properties of the central part

Using the TRANK program based on the DFT + GF method [37], we calculate the transport properties of the central part of the CNT-DV systems. The calculated transmission functions $T(E)$ under zero bias are plotted in figure 6. The $T(E)$ of 0 nN system shows a plateau near the Fermi level, while the 50 nN system presents a valley there, both being lower than that of a perfect CNT. We also calculate the electronic current under a bias of 0.1 eV. The corresponding conductances of 0 and 50 nN systems are $1.49G_0$ and $0.52G_0$, respectively, both being less than the value $2G_0$ of a perfect CNT. These results are consistent with the fact that in experiments the double vacancy can lower the current noticeably [17]. Furthermore, our calculation indicates that a large external force will lower the current more.

The different transport properties between 0 and 50 nN systems can be explained as follows. The conductance of the metallic CNT is mainly contributed by the conjugated π bonds originating from the p_z orbital of carbon atoms. The vacancy may break the conjugated network and therefore lower the conductance. For the 50 nN system, new bonds are formed and the overall conjugation is largely broken. As a result, the function $T(E)$ shows a deep valley near the Fermi energy, while for the 0 nN system, there is no new bond formed and the structure changes only little from the perfect CNT. Consequently, the break of the overall conjugation is smaller,

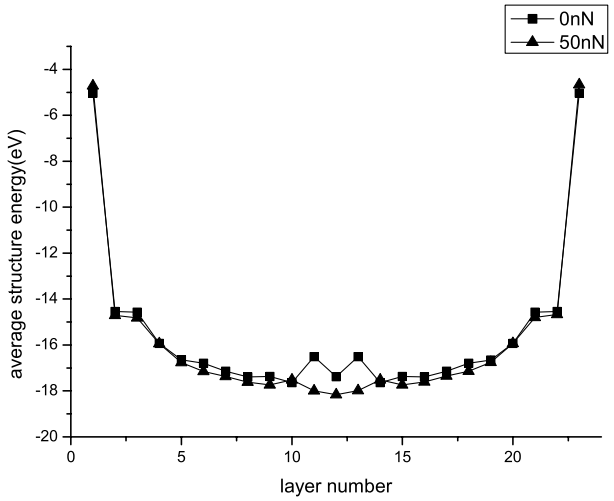

Figure 5. Average structural energies of the CNT-DV systems under 0 nN (denoted by square) and 50 nN (denoted by triangle) external forces.

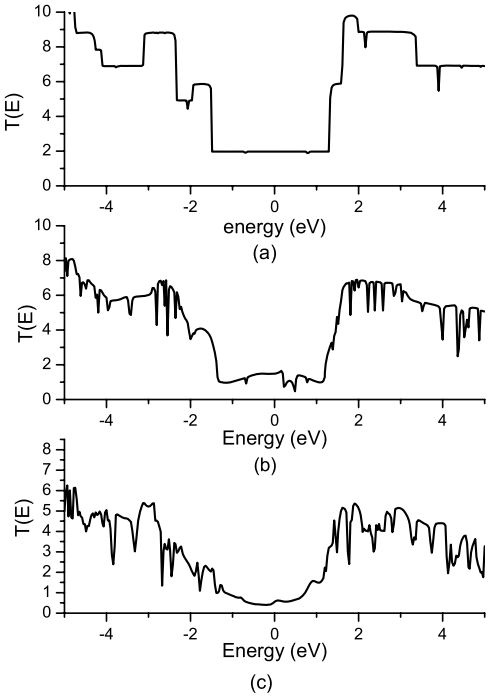

Figure 6. Transmission functions of the CNT-DV systems under (b) 0 nN and (c) 50 nN. The Fermi energy is set to be zero. (a) shows the transmission function of a perfect CNT for comparison.

resulting in a better electron transmission than the 50 nN system. Note that the difference in the conjugated π bonds for the two systems can also be seen from the analysis of LDOS above.

4. Conclusion

We have studied a (5, 5) carbon nanotube with a double vacancy under different external forces. The structure is optimized by the hybrid method combining the first-principles DFT and classical molecular dynamics calculations. Without the external force, the positions of the atoms change little from the perfect CNT. Under 50 nN external force, new bonds are formed along the circumference of the tube around the vacancy. The critical force for the transition is at 33–34 nN. This reconstruction cannot be predicted by classical molecular dynamics without a quantum description. The average structure energy analysis for each layer of the CNT show that the double vacancy has a very localized effect.

We have used the DFT + GF method to study the transport properties of the CNT-DV system. The defect reduces the transmission function $T(E)$ around the Fermi energy. Without the external force, $T(E)$ presents a plateau around the Fermi energy, while it shows a valley under the external force of 50 nN. Therefore, the double vacancy will lower the small bias current and the introduction of an external force will lower it further. This is consistent with the orbital analysis which shows that the HOMO of the 50 nN system is a local state, therefore blocking electron transport.

Acknowledgments

This work is supported by the NSFC (90306016) and by the '973' Project from the Ministry of Science and Technology of China (grant no. 2006CB605102).

References

[1] Jamieson V 2000 *Phys. World* **13** 29
Schönenberger C and Forró L 2000 *Phys. World* **13** 37
[2] Baughman R H, Zakhidov A A and de Heer W A 2002 *Science* **297** 787
[3] Dresselhaus M S, Dresselhaus G and Avouris Ph (ed) 2001 *Carbon Nanotubes: Synthesis, Structure, Properties and Applications* (*Springer Topics in Applied Physics* vol 80) (Berlin: Springer)
[4] Tombler T W and Zhou C W 2000 *Nature* **405** 769
[5] Kane C L and Mele E J 1997 *Phys. Rev. Lett.* **78** 1932
[6] Chico L, Crespi V H, Benedict L X, Louie S G and Cohen M L 1996 *Phys. Rev. Lett.* **76** 971
[7] Crespi V H, Cohen M L and Rubio A 1997 *Phys. Rev. Lett.* **79** 2093
[8] Nardelli M B 1999 *Phys. Rev.* B **60** 7828
[9] Nardelli M B and Bernholc J 1999 *Phys. Rev.* B **60** R16338
[10] Maiti A, Svizhenko A and Anantram M P 2002 *Phys. Rev. Lett.* **88** 126805
[11] Lu J-Q, Wu J, Duan W, Liu F, Zhu B-F and Gu B-L 2003 *Phys. Rev. Lett.* **90** 156601
[12] He Y, Zhang Ch, Cao Ch and Cheng H-P 2007 *Phys. Rev.* B **75** 235429
[13] Pierard N, Fonseca A, Konya Z, Willems I, Van Tendeloo G and Nagy J B 2001 *Chem. Phys. Lett.* **335** 1
[14] Ni B and Sinnott S B 2000 *Phys. Rev.* B **61** R16343
[15] Terrones M, Banhart F, Grobert N, Charlier J-C, Terrones H and Ajayan P M 2002 *Phys. Rev. Lett.* **89** 075505
[16] Choi H J, Ihm J, Louie S G and Cohen M L 2000 *Phys. Rev. Lett.* **84** 2917
[17] Gómez-Navarro C, De Pablo P J, Gómez-Herrero J, Bile B, Garcia-Vidal F J, Rubio A and Flores F 2005 *Nat. Mater.* **4** 534
[18] Landauer R 1970 *Phil. Mag.* **21** 863
[19] Datta S 1995 *Transport in Mesoscopic Systems* (Cambridge: Cambridge University Press)

[20] Hamada N, Sawada S I and Oshiyama A 1992 *Phys. Rev. Lett.* **68** 1579
[21] Mintmire J W, Dunlap B I and White C T 1992 *Phys. Rev. Lett.* **68** 631
[22] Saito R, Fujita M, Dresselhaus G and Dresselhaus M S 1992 *Appl. Phys. Lett.* **60** 2204
[23] Terrones M, Terrones H, Banhart F, Charlier J-C and Ajayan P M 2000 *Science* **288** 1226
[24] Mikó Cs, Milas M, Seo J W, Couteau E, Barišić N, Gaál R and Forró L 2003 *Appl. Phys. Lett.* **83** 4622
[25] Amorim R G, Fazzio A, Antonelli A, Novaes F D and da Silva A J R 2007 *Nano Lett.* **7** 2459–62
[26] Wang C Y and Zhang X 2006 *Curr. Opin. Solid State Mater. Sci.* **10** 2–14
[27] Zhang X and Wang C Y 2008 to be submitted
[28] Delly B 1990 *J. Chem. Phys.* **92** 508
Delly B 1998 *J. Quantum. Chem.* **69** 423
[29] Perdew J P, Burke K and Ernzerhof M 1996 *Phys. Rev. Lett.* **77** 3865
[30] Tersoff J 1988 *Phys. Rev.* B **37** 6991
[31] Tersoff J 1988 *Phys. Rev. Lett.* **61** 2879
[32] Brenner D W 1990 *Phys. Rev.* B **42** 9458
[33] Robertson D H, Brenner D W and Mintmire J W 1992 *Phys. Rev.* B **45** R12592
[34] Yakobson B I, Brabec C J and Bernholc J 1996 *Phys. Rev. Lett.* **76** 2511
[35] Nardelli M B, Yakobson B I and Bernholc J 1998 *Phys. Rev. Lett.* **81** 4656
[36] Kolmogorov A N and Crespi V H 2000 *Phys. Rev. Lett.* **85** 4727
[37] Ke S-H, Baranger H U and Yang W 2004 *Phys. Rev.* B **70** 85410
[38] Troullier N and Martins J L 1991 *Phys. Rev.* B **43** 1993
[39] Soler J M, Artacho E, Gale J D, Garcia A, Junquera J, Ordejón P and Sánchez-Portal D 2002 *J. Phys.: Condens. Matter* **14** 2745
[40] Ke S-H, Baranger H U and Yang W 2007 *J. Chem. Phys.* **127** 144107
[41] Mayer I 1986 *Int. J. Quantum Chem.* **29** 477